GEOTECHNICAL CHARACTERIZATION OF ALISOL SOILS IN EASTERN PROVINCE OF ZAMBIA

[1]Marsheal Fisonga, [2]Elvis Korir, [1]Patrick Chipola, [1]Victor Mutambo

[1]Department of Mining Engineering, School of Mines, University of Zambia, Great East Road Campus, P.O. Box 32379, Lusaka 10101, Zambia.
[2]Belgravia Services Limited.

DOI:10.53974/unza.jonas.6.1.483

ABSTRACT

In this study, the geotechnical characterization of the soils within the Mutenguleni area was investigated for the construction of the 2000m^3 fuel tank of the Chipata fuel deport. The soils within the tank farm exhibited a high presence of expansive clay minerals and low bearing capacity. Therefore, there was a need to investigate its characteristics and the soil improvement techniques to be implemented. The Zambian agricultural soil classification was used as the foundation to investigate the behaviour of active clay minerals found in the study area. The ***X-ray diffractometer (XRD)*** *Rietveld analysis depicted the presence of vermiculite, montmorillonite and Ferrum related minerals which are typical of alisols soils. The grain size analysis, Atterberg limits, Califonia bearing ratio (CBR), direct shear test, undrained unconsolidated triaxial test, and consolidation Oedometer were carried out. The CBR test also showed potential swelling and shrinkage behaviour of the investigated alisols soils. Based on the Casagrande plasticity chart the alisol soils from Chief Madzimawe of Eastern province can be classified as soil with low and high plasticity based on the soil horizon or presence of termite mould in the study area.*

Keywords: *Alisol soil, Expansive Clay Mineral, Soil classification*

INTRODUCTION

The alisol soil is characterized as one of the acidic soils and has high active clay minerals in their subsoil(Chesworth, 2008). Alisols are commonly found in subtropics, humid tropics and warm temperate areas with energetic acute weathering(Schaetzl and Anderson, 2005). Alisols soils depict great weathering of primary minerals, loss of silica and formation of new clay minerals as a consequence of the transformations in weathering by-products(Jordanova, 2016; Schaetzl and Anderson, 2005).

Geology of the area of study

The geology of Chipata is one of the most distinct and lithologically complex of all the terrains. It consists predominantly of variable retrogressed mafic, felsic and pelitic granulite, with subordinate hornblend, biotite, gneiss, variable deformed and under formed syenite. The geology age of Eastern Province of Zambia is comprised of the Karoo (Upper Carboniferous to Jurassic), Lithological units of various ages, Muva, Precambrian rocks of uncertain age-possibly Muva, probably largely older Precambrian and Tertiary to recent. The Chipata terrain is comprised of metamorphic monazite from pelitic granulite which is dated at circa 1046 Ma(Karmakar and Schenk, 2016). The granite is crosscut and retrogressed along high strain amphibolite-faces shear zones. The contact zones between the granulite and the lower-grade hornblende and biotite gneisses are not exposed with an unclear relationship between them. According to Johnson et al., the lower-grade gneisses are known to be a product of the highly deformed K-feldspar-bearing porphyritic augen granite(Johnson et al., 2006). Limited geochemical data indicate that the augen gneisses are calc-alkaline whereas the mafic amphibolite suggests formation in a continental extension setting(Johnson et al., 2006). Sometimes isolated outcrops of under formed K-feldspar-bearing porphyritic granite and garnet-bearing pelitic migmatite are present although their interaction with the surrounding granulite and gneiss(Johnson et al., 2006). The geological age from the investigated site was large older Precambrian as shown in Figure 1.

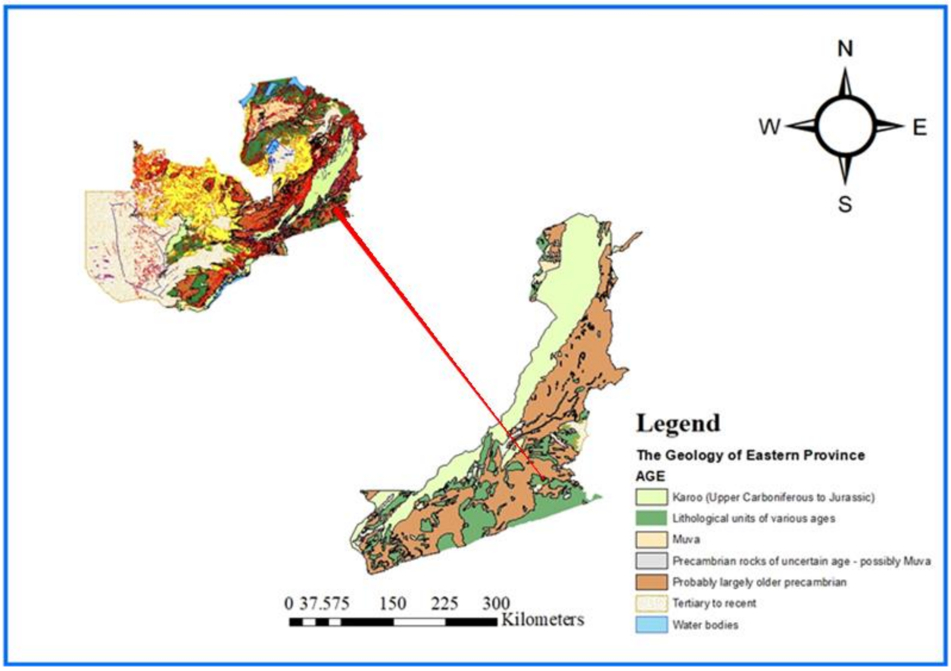

Figure 1 The geology of Eastern Province of Zambia

Soil Classification

In Zambia, extensive works on agricultural soil classification have been conducted extensively (Iwmi et al., 2005; Maki, 2008). However, the clay minerals and the geotechnical characterization of deformable geomaterials have not been investigated to mitigate the impact derived by climate change for the construction of storey buildings and mega infrastructures. Moreover, the rising sea levels and climate change around the globe have started showing effects in countries that have not been affected by natural phenomenons like Earthquakes, Cyclones and Tsunamis for a long time. On the other hand, most cities in Southern Africa are experiencing urbanisation at a very fast rate (UNDESA, 2010), which in turn requires the construction of storey buildings to maximise land utilization. Because of that, there is a need to pay attention to geotechnical characteristics of soils to reduce the infrastructure vulnerability from the phenomenon derived by the impact of climate change, rising sea levels, high pore water pressure and problematic soils. For instance, during the cyclone, Idai in Malawi, Mozambique and Zimbabwe suffered infrastructure vulnerability (Chapungu, 2020; Charrua et al., 2021; Concern Worldwide, 2021). Although the impact of these natural phenomena cannot be eliminated completely, some of the causes of building collapses are lack of good-engineered materials, design and geotechnical investigation before their construction (Asante and Sasu, 2018; Bamigboye et al., 2019; Chendo and Obi, 2015; Okagbue et al., 2018; Olusola and Akintayo, 2009; Teme et al., 2008). Because of limited knowledge on the geotechnical characterization in the majority in Southern African countries. However, the low-income communities may not be prepared to construct coastal infrastructure that can withstand the extreme forces derived by oceanic storms and incremental pore water pressure as a result of flooding caused by torrential rainfall.

In geotechnical engineering, water is known to be one of the common enemies of infrastructures constructed on or beneath the earth (Hall and Djerbib, 2004; Medero et al., 2011). Water can be in the form of moisture ingress and flooding(Berge, 2009). Flooding is one of the common outcomes of climate change(Medero et al., 2011). In addition, the occurrence of cyclones are accompanied by flooding which may lead to the increased porewater pressure destroying the soil bearing capacity(Fitchett, 2019; Wada, 2016). Furthermore, wetting and drying cause changes in the strength and stiffness of infrastructure walls (Medero et al., 2011). The study site in this research is located near the Makungwa weir with the high-water table at 1.2m from the surface within the vicinity of the foundation of the Chipata fuel depot tank farm.

This research focuses on investigating the geotechnical characterization of Alisol soil within Chief Madzimawe of Mutenguleni area 30km before Chipata from Lusaka for the construction of the Chipata Fuel Depot. This investigation was undertaken to mitigate the vulnerability of the foundation failure of the Chipata Fuel Depot from flooding caused by torrential rainfall, Swelling of the soil and the high-water table as a result of the nearby Makungwa weir. Apart from that, the failure of the foundation can cause the buckling of the fuel tank which may result in fuel tank failure causing soil pollution, underground water and Makungwa weir water pollution from the hydrocarbons. The objectives of this study are (i) to utilize the Zambian agricultural soil classification as the foundation of geotechnical Zambian soil Classification, (ii) investigate high active clays minerals through the implementation of XRD, and (iii) to classify the alisols soils from Chief Madzimawe of Mutenguleni area based on geotechnical characterization.

MATERIALS AND METHODS

The existing georeferenced database of Zambian soil classification-based Food and Agricultural Organization (FAO) was used as the foundation of this research. The determination of particle size distribution was undertaken according to (BS EN ISO 17892-4, 2014), Atterberg limits were determined according to(BS EN ISO 17892-12, 2018), The determination of the natural water content was done in line with (BS EN ISO 17892-1, 2014), the direct shear test was undertaken under Consolidated Drained Conditions in line with (ASTM-D3080/D3080M-11, 2020), the Unconsolidated-Undrained Triaxial Compression test of cohesive soils was undertaken based on (ASTM-D2850 − 15, 2015), the compaction of soils was done according to (BS1377: Part 4, 2003), and the consolidation test was undertaken accordance with(BS1377: Part 5, 1990). The classification of the soils will be done according to the Unified Soil Classification (USC) (ASTM D2487-11, 2006). The traces of expansive clay minerals such as montmorillonite, beidellite, chlorite, attapulgite, nontronite and vermiculite a basic expansive mineral in the samples from the site were investigated using XRD. Olympus TERRA-538 a portable X-ray fluorescence (XRF) and XRD equipment was used to carry the testing at a step of $2\theta^{o}=0.02^{o}$. Panalytical X'pert HighScore Plus software was used to analyze the X results. Table 1 shows the UTM coordinates of the sampled location from the study area and Figure 2 depicts the location within the Zambian Agricultural Soil Classification. The Tables 2-12 shows the feel and visual analysis of the Alisol soil from Chief- Madzimawe.

Table 1 Sampled location projection system WGS1984 Zone 36S

Trial Pit	Eastings	Northings	Elevation
TP001	439456	8477690	982
TP002	439351	8477646	982
TP003	439442	8477638	979
TP004	439483	8477600	982
TP005	439508	8477709	983
TP006	439526	8477732	984
TP007	439474	8477734	989
TP008	439495	8477758	989
TP009	439539	8477790	988
TP010	439594	8477792	986
TP011	439690	8477725	987

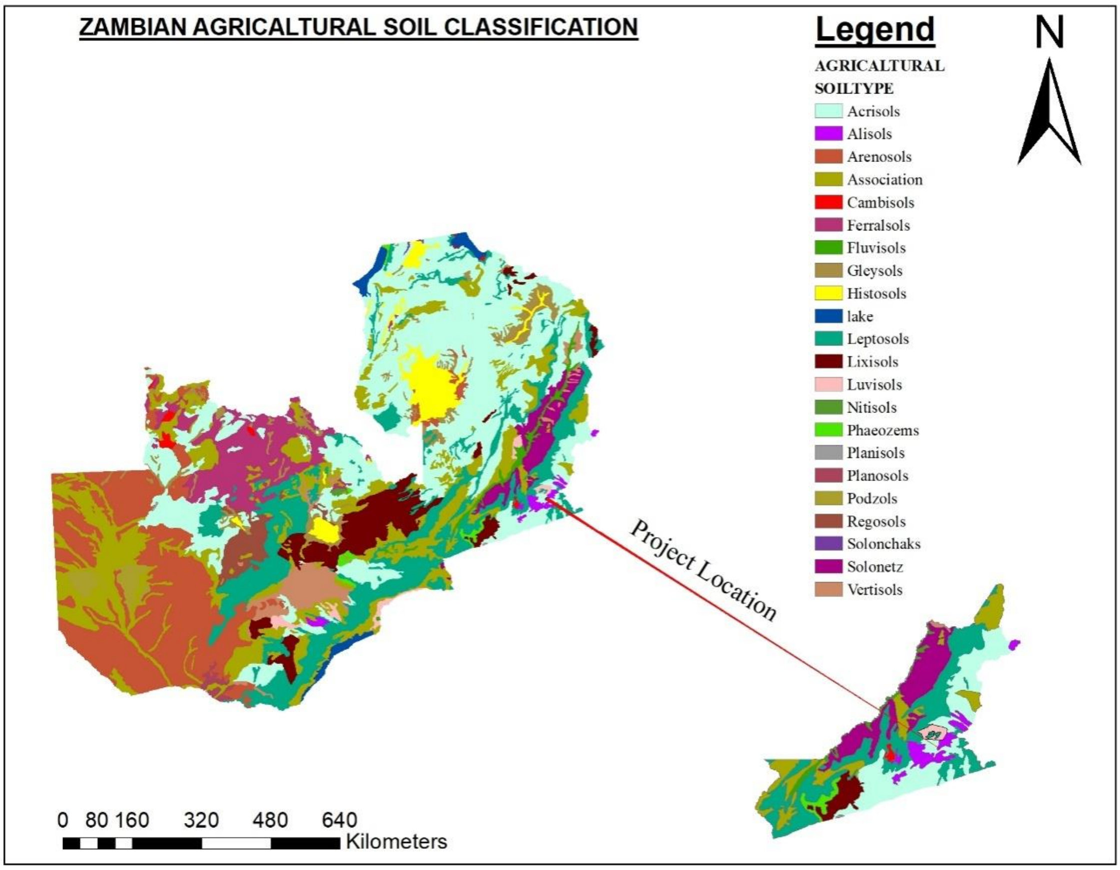

Figure 2 Location of the study area based on Zambian Agricultural Soil Classification

Table 2 description of soil for trail pit number one

TR001						
Collar Information						
Eastings	439456		Northings	8477690	Elevation	982
Logging						
Strip log	Elevation (m)	Depth (m)	Description			
	982	0				
	981.3	0.7	Dark grey humic soil with grassroots			
	978.95	2.35	A-horizon of dusky clayey soil with orange mottles			
	975.95	3	The water table intersected at 1.2m			

Table 3 description of soil for trail pit number two

TR002						
Collar Information						
Eastings	439351		Northings	8477646	Elevation	982
Logging						
Strip log	Elevation (m)	Depth (m)	Description			
	982	0				
	981.7	0.3	Humus-dusky brown with plants and grassroots.			
	980.7	1	A-horizon of dusky brown silty clayey soil			
	980.2	1.5	B- horizon dusky brownish red lateritic gravel			
	977.7	2.5	Water table intersected at 2.5m Yellowish-brown saprolitic clayey soil probably after a leucocratic gneiss			

Table 4 description of soil for trail pit number three

TR003						
Collar Information						
Eastings	439442		Northings	8477638	Elevation	979
Logging						
Strip log	Elevation (m)	Depth (m)	Description			
	979	0				
	977.5	1.5	B-horizon dusky reddish-brown lateritic gravelly soil			
	975.4	2.1	C-horizon light grey quartz-bio-musc saprolitic, probably after gneissic unit water intersected			

Table 5 description of soil for trail pit number four

TR004							
Collar Information							
Eastings	439493		Northings	8477600	Elevation	982	
Logging							
Strip log	Elevation (m)	Depth (m)	Description				
	982	0					
	981.6	0.4	Humus- dark grey soil with grass and plant roots				
	979.1	2.5	B-horizon of dusky reddish-brown lateritic gravelly soil				
	976.1	3	C-horizon with whitish-grey quartz-bio-musc silty clayey saprolitic horizon probably after gneissic unit. The water table intersected.				

Table 6 description of soil for trail pit number five

TR005							
Collar Information							
Eastings	439508		Northings	8477709	Elevation	983	
Logging							
Strip log	Elevation (m)	Depth (m)	Description				
	983	0					
	982.4	0.6	Humus-gravelly and rocks with plant roots				
	980.4	2.5	B-horizon of dusky reddish-brown lateritic gravelly soil				
	977.4	3	C-horizon with yellowish-brown limonitic silty clayey saprolitic horizon probably after gneissic unit.				

Table 7 description of soil for trail pit number six

TR006							
Collar Information							
Eastings	439428		Northings	8477732	Elevation	984	
Logging							
Strip log	Elevation (m)	Depth (m)	Description				
	984	0					
	983.55	0.45	Humus-dusky grey humic soil with plant roots				
	980.85	2.7	B-horizon with dusky reddish-brown lateritic gravelly soil				

	977.85	3	C-horizon with light grey clayey saprolitic horizon probably after gneissic unit.

Table 8 description of soil for trail pit number seven

TR007						
Collar Information						
Eastings	439474		Northings	8477734	Elevation	989
Logging						
Strip log	Elevation (m)	Depth (m)	Description			
	989	0				
	988.6	0.4	Humus-dusky brown gravelly humic soil with grass and plant roots.			
	986.6	2	B-horizon with dusky reddish-brown lateritic gravelly soil			
	983.6	3.1	C-horizon with medium grey fine-coarse grained grey clayey upper saprolitic horizon probably after gneissic unit.			

Table 9 description of soil for trail pit number eight

TR008						
Collar Information						
Eastings	439495		Northings	8477758	Elevation	989
Logging						
Strip log	Elevation (m)	Depth (m)	Description			
	989	0				
	988.6	0.4	Humus-dusky grey humic soil with grass and plant roots.			
	987.95	0.65	A-horizon with dusky reddish-brown silty clayey soil			
	986.75	1.2	A-horizon reddish-brown silty clayey soil.			
	984.5	2.5	B-horizon reddish brown gravelly lateritic soil.			
	981.25	3	C-horizon yellowish-brown clayey upper saprolite			

Table 10 description of soil for trail pit number nine

TR009						
Collar Information						
Eastings	439539		Northings	8477790	Elevation	988
Logging						
Strip log	Elevation (m)	Depth (m)	Description			
	988	0				
	987.5	0.5	Humus-dusky grey humic soil with grass and plant roots.			
	986.4	1.1	A-horizon with dusky grey silty clayey soil			

	983.4	3	B-horizon with reddish-brown gravelly lateritic soil.

Table 11 description of soil for trail pit number ten

TR010						
Collar Information						
Eastings	439594		Northings	8477792	Elevation	986
Logging						
Strip log	Elevation (m)	Depth (m)	Description			
	986	0				
	985.65	0.5	Humus-dusky grey humic soil with plant roots.			
	984.85	0.8	A-horizon with dusky grey silty clayey soil			
	983.15	1.7	B-horizon light grey silty clayey soil.			
	980.65	2.5	C-horizon with dusky reddish-brown gravelly soil with a very coarse-grained unit at the base.			
	977.65	3	C-horizon yellowish-brown clayey saprolite probably after gneissic unit.			

Table 12 description of soil for trail pit number ten

TR011						
Collar Information						
Eastings	439690		Northings	8477725	Elevation	987
Logging						
Strip log	Elevation (m)	Depth (m)	Description			
	987	0				
	986.7	0.3	Humus-dusky grey humic soil with plant roots.			
	985.4	1.3	Creamy medium coarse-grained fractured quartz-biotite-muscovite leucocratic gneiss.			

RESULTS AND DISCUSSION

Mineralogical soil classification

The classification of soil within the investigated area according to the Zambian agricultural soil classification is known to be the Alisols. Alisols have a higher clay content in the subsoil than in the topsoil as a result of clay migration (Jones et al.; 2013). Alisols are comprised of a low base saturation at certain depths and high-activity clays such as illite, montmorillonite and vermiculite in the clay-rich horizon (Jones et al.; 2013). The acidity of the alisol soils is caused by the weathering of minerals which release a large amount of aluminium (Jones et al.; 2013). They occur predominantly in humid tropical, humid subtropical and warm temperate regions. The present high-activity clay minerals are as a result of weathering under the present humid conditions in the area which in turn causes the intense leaching of silica, alkaline and alkaline-earth cations. Besides, Alisols are highly dominated by shrinkage-swelling minerals. Aluminium is known to be occupying more than 50% of the exchange complexes. In this study, the presence of the subgroups of the active clay minerals of smectite such as montmorillonite and vermiculite a basic expansive mineral were found present from the XRD analysis in high contents. The subsoil had a high presence of deep in-situ weathered saprolite with the vermiculite basic mineral present. The presence of vermiculite is as a result of the weathered gneiss which contains the mica subgroups such as the phlogopite, phengite and muscovite(Hillel, 2005). In this area, the mica minerals such as phlogopite, phengite, muscovite, etc. are highly present. The reddish colour in the soils of this geological formation is as a result of the high amount of Ferrum (Fe) content in the subsurface. The saprolite is normally clayey because of the weathered feldspars and ferromagnesian to clay minerals like montmorillonite. The Alisols soils in the study area belong to the temperate, dry winter, hot summer (Cwa) (Rao, 2008). Therefore, although there is some exposure of the gneiss rocks within the vicinity of the construction site, the depth of the bedrock below the surface for this type of soil formation was encountered at 12m during the coring.

X-ray powder diffraction (XRD)

XRD analysis depicted the presence of Achavalite, Albite, Anorthoclase, Annite, Atokite, Birnessite, Bixbyite, Braunite, Bytownite, Calcirtite, Chloritoid, Garronite, Guidottite, Grimalddite, Ferrihydrite, Ferrotapiolite, Heklaite, Lizardite, Martyite, Matulaite, Melanovanadite, Montmorillonite, Muscovite 2M1, Pyrochroite, Ramsdellite, Richetite, Tapiolite, Tazheranite, Titanium, Vermiculite and Wuestite from the samples. The investigation of high active clay (HAC) in the Chipata alisols soils showed traces of vermiculite and montmorillonite. Vermiculite is a metastable expansive mineral. Figure 3 shows the Rietveld results from one of the specimens investigated. The presence of vermiculite and montmorillonite in alisols soils agrees well with the findings of the previous researchers (Jones et al.; 2013). On the other hand, the presence of Tapiolite, Ferrotapiolite and Ferrihydrite were as a result of high Fe content in the investigated soil. The soils from the study area also contained portlandite which is a clear indication that the soils within the study area have hydration capabilities, hence, their stabilization at a minimal cement dosage would be adequate.

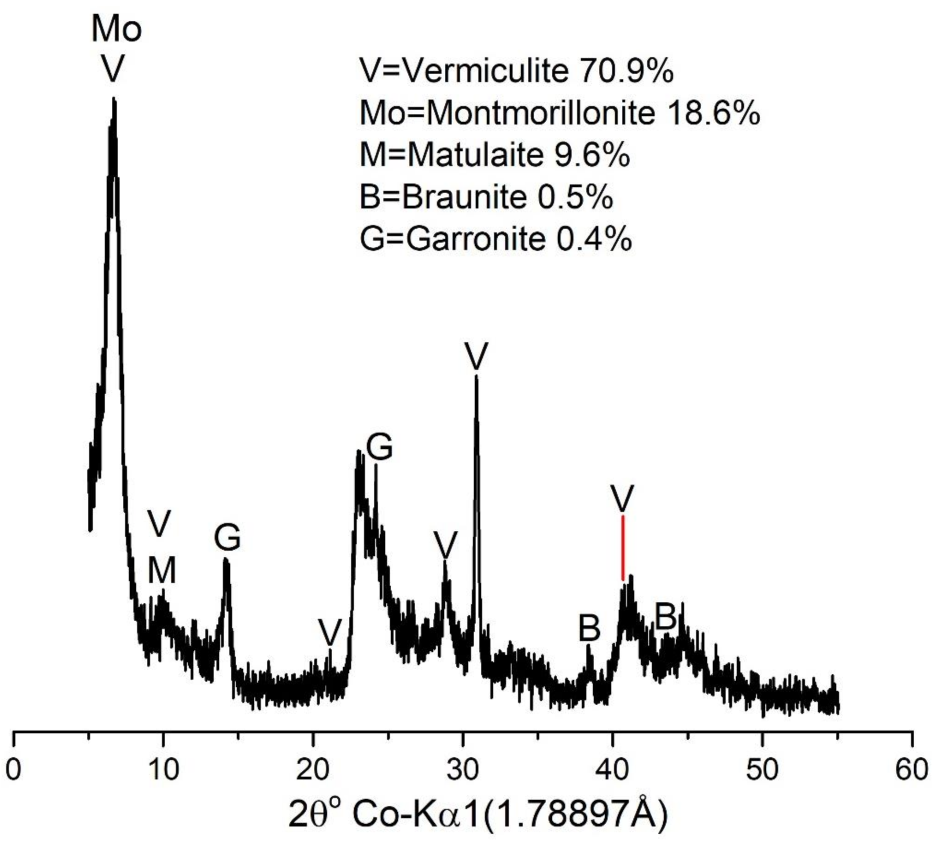

Figure 3. XRD analysis for TP002 3-4m specimen

Physical properties of the soils

The soils that showed high plasticity was seen to be from the B and C-horizons. On the other hand, the soil sample TR010A was also depicted to be of high plasticity and this was because the trail pit for this sample was within the premises of the termite mound. The findings are in line with (Assam et al., (2016) results. The high natural moisture content determined was because of the high-water table within the area of the construction site. The high-water table within the area is because of the meandering stream on the southwest of the construction site and the existence of the Makungwa weir on the north-western side of the construction site. The unstabilised compacted B and C-horizon soils at 2% plus the optimum water content showed a lower Califonia Bearing Ratio (CBR). However, it was found that if the lateritic soils from the same site are stabilized at 3% cement dosage the CBR of 100% was attained. The CBR results for unstabilised soils showed the swelling potential of the studied soils this was as a result of the high plastic clays in the area containing expansive clay mineral montmorillonite and vermiculite (Faezehossadat and Jeff, 2016). Therefore, the more water absorbed by the alisols soils from the construction site the higher the swelling (Faezehossadat and Jeff, 2016). Tables 13 to 15 shows the physical properties of the investigated soils(ASTM D2487-11, 2006), Figure 4 represents the Casagrande chart of the investigated soil (ASTM D2487-11, 2006). The cohesion and friction angle of the dominant saprolite soils from the direct shear and undrained unconsolidated (UU) triaxial test are shown in Table 16. Besides, Figure 5 and Table 17 shows the results of the undisturbed soil consolidation test.

Table 13 Characteristics of the soils from TR002A, TR002B, TR003B and TR003C

	TR002A	TR002B			TR003B	TR003C		
Percentage of Gravel (%)	37.82	16.81			12.53	3.37		
Percentage of Sand (%)	32.42	42.77			47.47	54.89		
Percentage of Silt & Clay (%)	29.75	40.42			40	41.74		
Liquid Limit LL (%)	40.5	49.2			47.1	34		
Plastic Limit (PL)	13.1	22.5			21.5	15.6		
Plasticity Index (%)	27.3	26.7			25.7	18.4		
Natural Moiture Content (%)	15.7	33.5			18.8	20.4		
Linear Shrinkage, LS=100*(1-(LD/LD)) (%)	14.21	12.56			11.43	9.71		
Shrinkage Products, SP=LS*%<425um	504.81	722.04			594.29	624.63		
Group symbol	GC	SC			SC	SC		
ASTM designation as	Clayey Gravel with Sand	Clayey Sand with Gravel			Clayey Sand	Clayey Sand		
MDD (kg/m^3)	NA	1692			NA	2007		
OMC (%)	NA	17.7			NA	10.2		
Compaction (%)	NA	93	95	98	NA	93	95	98
CBR (%)	NA	3	3	4	NA	4	5	6
Swell (%)	NA	4.54	5.24	5.92	NA	2.83	2.91	3.24
Depth (m)	0.3 to 1	1 to 1.5			0.8 to 1.5	1.5 to 2.1		

High Active Clay	Montmorillonite (0.6-1m)	Vermiculite	x	x
		Vermiculite (2-4m)		

Table 14 Characteristics of the soils from TR004B, TR004C, TR006B and TR006C

	TR004B	TR004C			TR006B	TR006C		
Percentage of Gravel (%)	17.81	2.39			15.03	2.63		
Percentage of Sand (%)	31.61	56.69			41.54	30.54		
Percentage of Silt & Clay (%)	50.58	40.92			43.43	66.83		
Liquid Limit LL (%)	51.9	30.4			52.3	44.2		
Plastic Limit (PL)	23.6	18			26.5	20.2		
Plasticity Index (%)	28.3	12.4			25.8	24		
Natural Moiture Content (%)	21.6	18.9			13.4	24.9		
Linear Shrinkage, LS=100*(1-(LD/LD)) (%)	13.86	6.23			13.21	12.49		
Shrinkage Products, SP=LS*%<425um	827.27	371.85			705.64	1018.83		
Group symbol	CH	SC			SC	CL		
ASTM designation as	Sandy Fat Clay with Gravel	Clayey Sand			Clayey Sand with Gravel	Sandy Lean Clay		
MDD (kg/m^3)	NA	1980			NA	1835		
OMC (%)	NA	11.5			NA	16.1		
Compaction (%)	NA	93	95	98	NA	93	95	98
CBR (%)	NA	16	20	27	NA	3	4	5
Swell (%)	NA	0.45	0.83	1.16	NA	3.01	3.82	4.49
Depth (m)	0.4 to 2.5	2.5 to 3			0.45 to 2.7	2.7 to 3		

Table 15 Characteristics of the soils from TR007B-C, TR010A and TR010B-C

	TR007C	TR010A	TR010B-C
Percentage of Gravel (%)	13.45	7.35	22.81
Percentage of Sand (%)	40.53	33.61	49.49
Percentage of Silt & Clay (%)	46.01	59.04	27.7
Liquid Limit LL (%)	55.3	50.3	45.2
Plastic Limit (PL)	23.4	26.5	18.7
Plasticity Index (%)	31.9	23.9	26.5
Natural Moiture Content (%)	16.1	15	15.4
Linear Shrinkage, LS=100*(1-(LD/LD)) (%)	12.29	14	13.29
Shrinkage Products, SP=LS*%<425um	718.71	977.2	587.23
Group symbol	SC	CH	SC
ASTM designation as	Clayey Sand	Sandy Fat Clay	Clayey Sand with Gravel
MDD (kg/m^3)	NA	NA	1898
OMC (%)	NA	NA	14.1
Depth (m)	0.4 to 2	0.5 to 0.8	0.8 to 1.7

Compaction (%)	NA	NA	93	95	98
Neat CBR (%)	NA	NA	8	10	13
Swell (%)	NA	NA	1.17	1.43	2.06
Stabilized SPT10B samples					
Compaction (%)			93	95	98
Stabilized CBR (%)	2% Cement		65	54	46
Swell (%)			0.09	0.12	0.17
Compaction (%)			93	95	98
Stabilized CBR (%)			172	110	68
Swell (%)	4% Cement		0.04	0.07	0.09
Compaction (%)			93	95	98
Stabilized CBR (%)			300	254	222
Swell (%)	6% Cement		0.02	0.02	0.02
			Vermiculite (0 to 0.5m)		
			Montmorillonite (0.8 to 1.7m)		
High Active Clay Minerals			Montmorillonite (1.7 to 3m)		

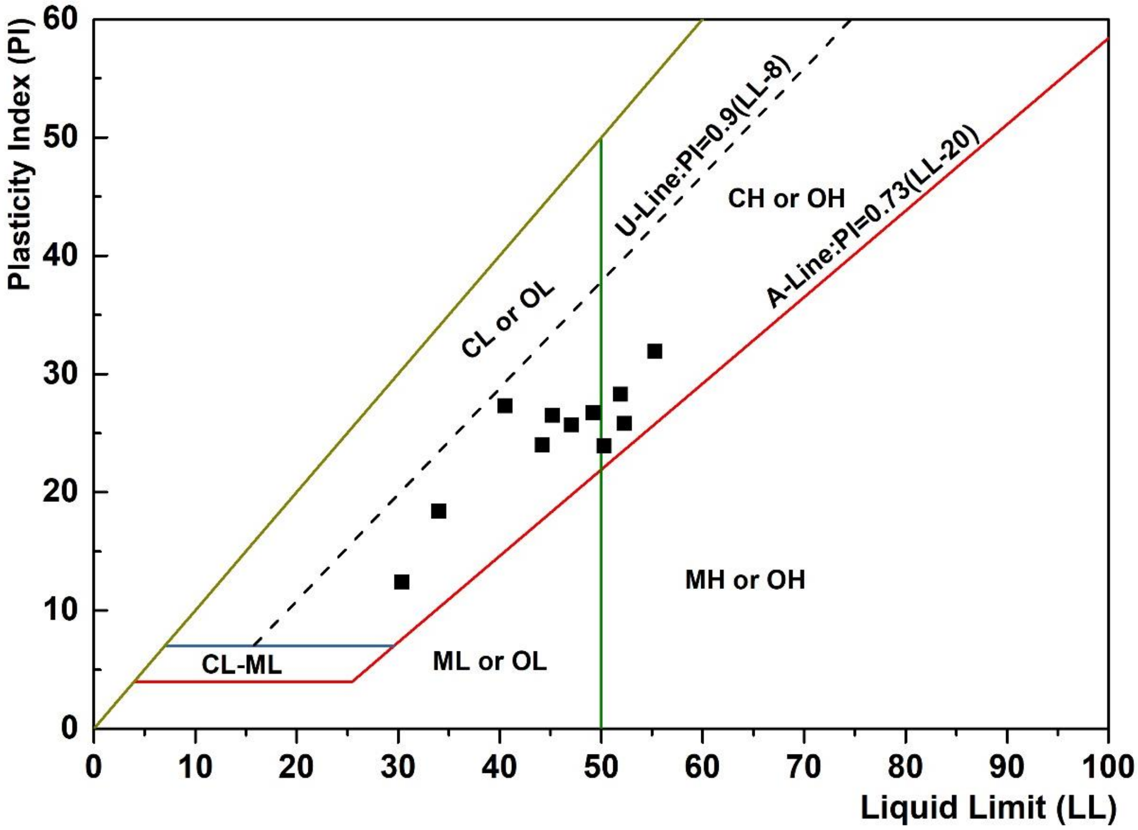

Figure 4 Casagrande chart

Table 16 Cohesion and Friction Angle of Undisturbed Soils

Direct Shear		UU Triaxial	
Cohesion (kPa)	Friction Angle ϕ (°)	Cohesion (kPa)	Friction Angle ϕ (°)
11.3	9.5	9.1	8.8

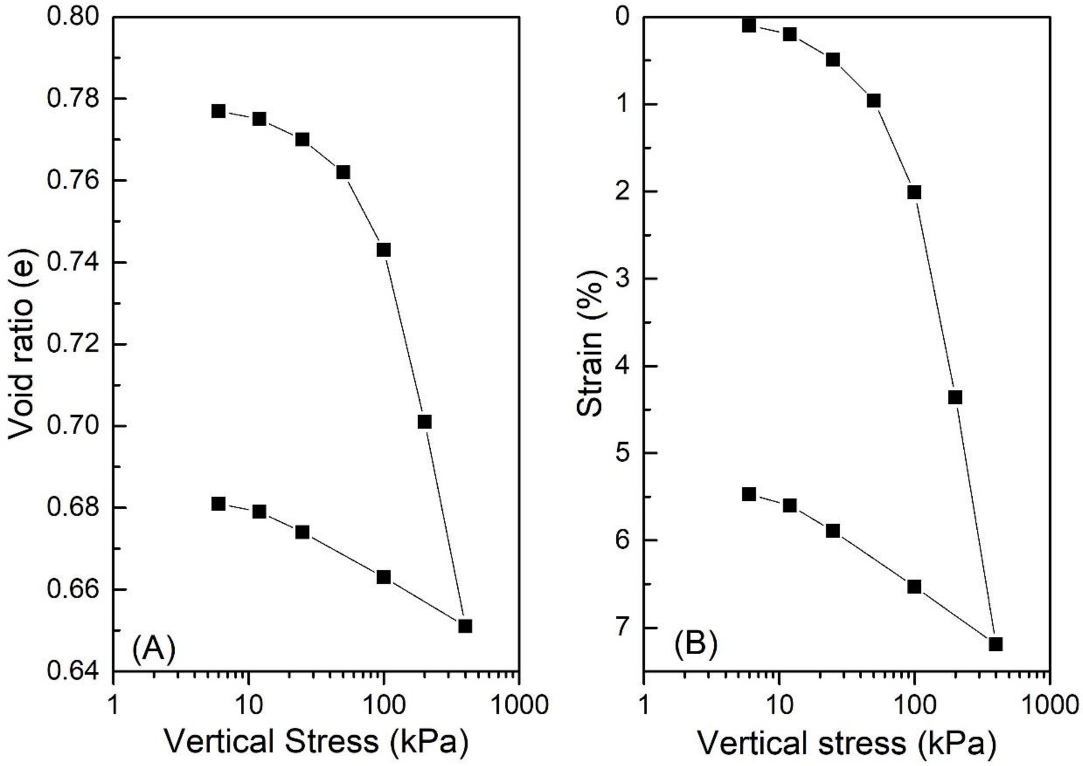

Figure 5 (A) Void Ratio vs Log Stress and (B) Strain vs Log Stress

Table 17Consolidation Test: Standard Oedometer

Sample Parameters		Unit	Value	Sample	Unit	Value	Remarks
Moisture Content	Before Test	%	25.6	The dry mass of the total specimen after testing	g	55.67	
	After Test	%	25.4	Moist mass of the specimen before the test	g	69.91	
Initial Dry Density		ρ_d(g/cm^3)	1.49	Moist mass of the specimen after the test	g	69.83	
Void Ratio before the test		-	0.78	Ring diameter	cm	5	
Degree of Saturation		%	89.4	Ring height	cm	1.9	
Initial Specimen Height		mm	19	Final sample height	cm	1.763	
Calculated Relative Density (SG)		-	2.65				Undisturbed Soil Sample

Test Parameters												
Vertical stress	kPa	6	12	25	50	100	200	400	100	25	12	6
Time Elapsed	hour	24	24	24	24	24	24	24	24	24	24	24
H_{100}	mm	18.985	18.962	18.907	18.818	18.619	18.172	17.633	17.76	17.88	17.937	17.961
ΔH	mm	0	0.04	0.093	0.182	0.3813	0.8277	1.367	1.24	1.12	1.063	1.039
Strain	%	0.1%	0.2%	0.49%	0.96%	2.01%	4.36%	7.19%	6.53%	5.89%	5.60%	5.47%
Void Ratio	-	0.777	0.775	0.77	0.762	0.743	0.701	0.651	0.663	0.674	0.679	0.681
m_v	m^2/MN	-	0.34	0.38	0.38	0.4	0.44	0.36				
$C_{v(t90)}$	m^2/year	-	59.92	25.81	25.79	44.56	54.82	36.51				
$C_{v(t50)}$	m^2/year	-	25.06	10.79	10.78	18.63	22.92	15.27				
Es	MPa	4.3										

The soils from the investigated site are disadvantaged for the construction of huge structures that will exert high pressure on the soils this is because of the presence of expansive clays, high water table and low bearing capacity in the upper soil horizons. The high water table within the area can lead to the development of high pore water pressure that can destroy the soil strength (Budhu, 2011; Das and Sivakugan, 2019). As the site lies within an area with a high-water table, deep soils and the presence of expansive clays, the soils in this area are likely to suffer from both the swelling and shrinkage behaviour. Therefore, when constructing huge structures special attention should be paid to the soil treatment so that the natural moisture content is not disturbed to trigger high expansion that may lead to high soil volume change which will result in structural buckling and uplift pressure (Zumrawi and Abdelmarouf, 2017). To control the swelling and shrinkage behaviour, the installation of horizontal barriers which will act as a blanket for the soil moisture fluctuation control should be considered (Zumrawi and Abdelmarouf, 2017). Besides, surface and subsurface drainage are of great importance in the control of moisture fluctuation (Zumrawi and Abdelmarouf, 2017).

CONCLUSIONS

The XRD analysis of the studied soils revealed that the soil within the construction site of the Chipata Fuel Depot was Alisol.

The XRD Retiveld analysis depicted that the Alisols soils within Chief Madzimawe of Mutenguleni area contained a high presence of Vermiculiteat 77.7% and Montmorillonite at 54.9%. The California bearing ratio (CBR) for the sample of TR002B, TR003B, TR004B, TR006C, and TR010C showed the swelling capabilities of the investigated soils which resulted from the presence of HAC.

Classification of the soil within the study area in line with the USC from the perspective of grain size analysis of the A-horizon was found to be dominant in group CH and GC, B-horizon was CH and SC, and C-horizon was CL and SC. On the Casagrande chart, the soils were plotting between the A-line and U-line from low plasticity to high plasticity.

RECOMMENDATION

Soils that exhibit swelling capability from the CBR test or develop cracks when dry their microstructure should be investigated using XRD and Scanning Electron Microscope.

Expansive soils should be stabilized to mitigate the detrimental effect that they pose to the civil structure to be constructed.

The soil from the study site has a low bearing capacity and the bedrock can be encountered at the depth between 15 to 30 m. Therefore, for heavy loading structures, a deep foundation should be used.

ACKNOWLEDGEMENTS

We would like to express our gratitude for the financial support from Belgravia Services Limited.

References

Asante, L.A., Sasu, A., 2018. The Challenge of Reducing the Incidence of Building Collapse in Ghana: Analyzing the Perspectives of Building Inspectors in Kumasi. SAGE Open 8. https://doi.org/10.1177/2158244018778109

Assam, S., Okafor, F., Umoh, U., 2016. Potentials of Processed Termite as a Stabilizing Agent in Clay Soil. IOSR J. Mech. Civ. Eng. 13, 40–50. https://doi.org/10.9790/1684-1304014050

ASTM-D2850 − 15, 2015. Standard Test Method for Unconsolidated-Undrained Triaxial Compression Test on Cohesive Soils. ASTM Int. D2850 − 15, 1–6. https://doi.org/10.1520/D2850-15.2

ASTM-D3080/D3080M-11, 2020. Standard test method for the direct shear test of soils under consolidated drained conditions. ASTM Int. 1–9. https://doi.org/10.1520/D3080

ASTM D2487-11, 2006. Standard Practice for Classification of Soils for Engineering Purposes (Unified Soil Classification System). ASTM Stand. Guid. D5521-05, 1–5. https://doi.org/10.1520/D2487-11.

Bamigboye, G.O., Michaels, T., Ede, A.N., Ngene, B.U., Nwanko, C., Davies, I., 2019. The Role of Construction Materials in Building Collapse in Nigeria: A Review. J. Phys. Conf. Ser. 1378. https://doi.org/10.1088/1742-6596/1378/4/042022

Berge, B., 2009. The ecology of building materials, 2nd ed. Elsevier.

BS EN ISO 17892-1, 2014. Geotechnical investigation and testing - Laboratory testing of soil. Determination of water content. Br. Stand. Inst.

BS EN ISO 17892-12, 2018. Geotechnical investigation and testing - Laboratory testing of soil. Br. Stand. Inst.

BS EN ISO 17892-4, 2014. Geotechnical investigation and testing — Laboratory testing of soil Part 2 : Determination of bulk density. Br. Stand. Inst.

BS1377: Part 4, 2003. Geotechnical investigation and testing — Laboratory testing of soil Part 4: Compaction-related tests. Br. Stand. Inst.

BS1377: Part 5, 1990. Geotechnical investigation and testing — Laboratory testing of soil Part 5: Compressibility, permeability and durability tests. Br. Stand. Inst.

Budhu, M., 2011. Soil Mechanics and Foundations, 3rd ed. JOHN WILEY & SONS, INC.

Chapungu, L., 2020. Mitigating the impact of cyclone disasters: Lessons from Cyclone Idai. Clim. Chang. Migr.

Charrua, A.B., Padmanaban, R., Cabral, P., Bandeira, S., Romeiras, M.M., 2021. Impacts of the tropical cyclone idai in Mozambique: A multi-temporal Landsat satellite imagery analysis. Remote Sens. 13, 1–17. https://doi.org/10.3390/rs13020201

Chendo, I.G., Obi, A.N.I., 2015. Building Collapse in Nigeria: the Causes, Effects, Consequences and Remedies. Int. J. Civ. Eng. Constr. Estate Manag. 3, 41–49.

Chesworth, W., 2008. Encyclopedia of soil science, Choice Reviews Online. https://doi.org/10.5860/choice.45-5914

Concern Worldwide, 2021. The impact of Cyclone Idai on the poorest. Concern Worldwide. 1–12.

Das, B.M., Sivakugan, N., 2019. Prinsiples of Foundation Engineering, 9th ed. CENGAGE.

Faezehossadat, K., Jeff, B., 2016. Expansive Soil: Causes and Treatments. i-manager's J. Civ. Eng. 6, 1. https://doi.org/10.26634/jce.6.3.8083

Fitchett, J., 2019. Tropical cyclone Idai: The storm that knew no boundaries [WWW Document]. News 24.

Hall, M., Djerbib, Y., 2004. Moisture ingress in rammed earth : Part 1 — the effect of soil particle-size distribution on the rate of capillary suction. Emerald Gr. Publ. Ltd. 18, 269–280. https://doi.org/10.1016/j.conbuildmat.2003.11.002

Hillel, D., 2005. Encyclopedia of Soils in The Environment. Elsevier.

Iwmi, A.N., Moody, P., Payne, W., 2005. Management of Tropical Sandy Soils for Sustainable Agriculture, in: FAO. Fa.

Johnson, S.P., De Waele, B., Liyungu, K.A., 2006. U-Pb sensitive high-resolution ion microprobe (SHRIMP) zircon geochronology of granitoid rocks in eastern Zambia: Terrane subdivision of the Mesoproterozoic Southern Irumide Belt. Tectonics 25. https://doi.org/10.1029/2006TC001977

Jones, A., Breuning-Madsen, H., Brossard, M., Dampha, A., Deckers, J., Dewitte, O., Gallali, T., Hallett, S., Jones, R., Kilasara, M., Le Roux, P., Micheli, E., Montanarella, L., Spaargaren, O., Thiombiano, L., Van Ranst, E., Yemefack, M., Zougmoré R., (eds.), 2013. Soil Atlas of Africa, FAO, Rome, Italy and IIASA, Laxenburg, Austria. European Commission, Publications Office of the European Union, Luxembourg. 176 pp. https://doi.org/10.2788/52319

Jordanova, N., 2016. Soil Magnetism: Applications in Pedology, Environmental Science and Agriculture, Soil Magnetism: Applications in Pedology, Environmental Science and Agriculture.

Karmakar, S., Schenk, V., 2016. Mesoproterozoic UHT metamorphism in the Southern Irumide Belt, Chipata, Zambia: Petrology and in situ monazite dating. Precambrian Res. 275, 332–356. https://doi.org/10.1016/j.precamres.2016.01.018

Maki, H., 2008. Agriculture and Forestry in Zambia. Japan Assoc. Int. Collab.

Medero, G.M., Kennedy, J.H., Woodward, P.K., Banimahd, M., 2011. Flooding Effect on Earth Walls. Sustainability 69–81. https://doi.org/10.3390/su3010069

Okagbue, H.I., Iroham, C.O., Peter, N.J., Owolabi, J.D., Adamu, P.I., Opanuga, A.A., 2018. A systematic review of building failure and collapse in Nigeria. Int. J. Civ. Eng. Technol. 9, 1391–1401.

Olusola, B.S., Akintayo, O., 2009. An assessment of the failure of building components in Nigeria. J. Build. Apprais. 4, 279–286. https://doi.org/10.1057/jba.2009.6

Rao, G.S.L.H.V.P., 2008. Agricultural Meteorology. PHI Learning Private Limited, Delhi-110092.

Schaetzl, R., Anderson, S., 2005. Soil Genesis and Geomorphology. Cambridge University Press, Cambridge.

Teme, S.C., Ngerebara, O.D., Geotechnical, T., Nig, C., Harcourt, P., 2008. Need for Prior Geotechnical Engineering Studies for Foundation Design : Cases of Collapsed Buildings in Port Harcourt and Environs, Nigeria. Science (80-.). 1–8.

UNDESA, 2010. World Urbanization Prospects The 2012 Revision New York. United Nations.

Wada, A., 2016. Excess pore water pressure and its impact, in: The 15th Asian Regional Conference on Soil Mechanics and Geotechnical Engineering. Japanese Geotechnical Society Special Publication, pp. 335–339.

Zumrawi, M., Abdelmarouf, A.O., 2017. Damages of buildings on expansive soils : diagnosis and avoidance damages of buildings on expansive soils : diagnosis and avoidance. Int. J. Multidiscip. Sci. Emerg. Res. 6, 108–115.